JOURNAL OF CATALYSIS 101, 169–177 (1986)

The Effect of Various Bimetallics on the Graphite–Steam Reaction

R. T. K. BAKER, J. A. DUMESIC,[1] AND J. J. CHLUDZINSKI, JR.

Exxon Research and Engineering Company, Clinton Township, Rt. 22 East, Annandale, New Jersey 08801

Received November 19, 1985; revised April 10, 1986

This study reports the use of bifunctional catalysts for the carbon–steam reaction, where one component increases the oxygen reactivity and the other component accelerates the supply of carbon from the source material to the catalyst–gas interface. The mixed catalysts selected for this purpose were nickel–titanium, nickel–platinum, nickel–ruthenium, and platinum–titanium. Using a combination of controlled atmosphere electron microscopy and flow reactor studies, we have found that the bimetallic systems exhibit a rate of catalytic attack of graphite in steam that is higher than either of the respective pure components. In addition to modifying the catalytic activity of a given metal, introduction of a second metal into the system can also produce changes in the wetting characteristics of the catalyst on graphite. In the presence of platinum, ruthenium, and mixtures containing these metals catalytic gasification occurs along the armchair edges of graphite. In all other systems studied here and previously, the receding edges are aligned parallel to the zigzag edges of graphite. A rationale is presented to account for this phenomenon which is based on the nature of the adsorption characteristics of water molecules on the catalyst surface and the chemical state of the prismatic faces of the graphite when reacted in steam.

INTRODUCTION

There are surprisingly few accounts in the literature of investigations pertaining to the use of bimetallics as catalysts for steam gasification of carbon. In an earlier controlled atmosphere electron microscopy study we showed that the strength of the interaction of nickel–iron particles with graphite in the presence of steam was less than that of nickel. As a consequence, catalytic attack by nickel–iron particles was restricted to the channeling mode, whereas gasification occurred with nickel by the more extensive edge recession mode. Despite this difference in behavior, the bimetallic was found to be a more active catalyst than either of its pure constituents for the graphite–steam reaction (*1*).

In a similar type of investigation, Lund and co-workers (*2*) developed the concept of a bifunctional catalyst for steam gasification of graphite. Using a platinum–barium catalyst they found a higher intrinsic catalytic activity than that exhibited by either of the single components for the graphite–steam reaction. They suggested that this result was due to barium increasing the oxygen reactivity, and platinum increasing the carbon reactivity.

Rao and co-workers (*3*) studied the effect of several nickel alloys on the gasification of graphite in a wet hydrogen environment ($H_2 : H_2O = 40 : 1$); however, under these conditions it is uncertain which would be the dominant carbon–gas reaction, carbon–hydrogen, or carbon–steam. For this reason, one must be cautious in interpreting the data presented in that paper.

In the present study, we have attempted to exploit the concept of a bifunctional catalyst for the graphite–steam reaction through the investigation of other mixed metal systems, including nickel–titanium, nickel–platinum, nickel–ruthenium, and platinum–titanium. Some of the electron microscopy investigations have been complemented with macroscale experiments performed in a flow reactor at higher pres-

[1] Chemical Engineering Department, University of Wisconsin, Madison, Wisc. 53706.

0021-9517/86 $3.00

sures than is possible in the CAEM technique (*4*).

II. EXPERIMENTAL

The bimetallics were introduced onto transmission specimens of single crystal graphite by a variety of methods. Nickel–titanium, nickel–platinum, and platinum–titanium were prepared by sequential deposition of the two metals onto the graphite substrates by evaporation of the respective spectrographically pure wires from a tungsten filament at a residual pressure of 10^{-6} Torr. The conditions were selected so as to produce approximately monolayer films of each component. Nickel–ruthenium was added as an atomized spray from an aqueous solution of the respective nitrates, mixed in amounts which would produce 1 : 1 ratios of each metal. Conditions of spraying were chosen so that, upon subsequent decomposition of the precursor salts, a mixed metal coverage of about two monolayers was obtained. Before reaction in a steam environment all specimens were treated at 600°C in 1.0 Torr hydrogen for 2.0 h to reduce all species to the metallic state.

The argon and hydrogen gases used in the microscopy section of this work were obtained from Scientific Gas Products, Inc. with stated purities of 99.999% and were used without further purification. Steam was introduced into the system by flowing argon through a gas saturator containing deionized water at 20°C, a procedure which produced an argon/water ratio of about 40 : 1 in the gas reaction cell.

The carbonaceous material used in the flow reactor studies was SP-1 graphite (Union Carbide). Ruthenium nitrate (research grade) was obtained from Engelhard Chemicals. Nickel nitrate and chloroplatinic acid, both research grade, were purchased from Alfa Chemicals. Metal/graphite samples containing 5 wt% metal were prepared by aqueous impregnation of the graphite using solutions of the respective salts to give 1 : 1 ratios of Ni : Pt and Ni : Ru. The impregnates were heated in a 10% hydrogen/argon stream at 500°C for 4 h to reduce all species to the metallic state before reaction with steam.

The apparatus used for these experiments has been described previously (*1*). The reactant gas was generated by bubbling an argon/0.5% hydrogen mixture through water at 25°C at a flow rate of ca. 0.8 cm^3/sec. Experiments were carried out at 600, 700, and 800°C, and estimates were made of the amount of carbon gasified after 2.0 h by weight loss measurements. For this purpose, the starting weight was taken as the initial sample weight, less the amount lost during the reduction treatment as found from blank experiments.

III. RESULTS

Controlled Atmosphere Electron Microscopy Studies

When the various bimetallic nickel/graphite specimens were heated in 2.0 Torr wet argon many common features were evident. Nucleation of small particles occurred at temperatures between 400 and 475°C and those which accumulated at edges and steps on the graphite were in a nonwetting state. Over the temperature range from 555 to 610°C, these particles exhibited a dramatic change in morphology, first wetting the surface and then proceeding to spread along the edge and step regions in the form of a thin film. The subsequent behavior of these "coated" graphite features was dependent on the chemical nature of the catalytic species and will be described under separate headings. To assist the reader with some of the descriptions of the catalytic action of the various bimetallics on the graphite, a schematic representation of the crystallographic directions and atomic planes with respect to the graphite basal plane are given in Fig. 1.

Nickel–Titanium/Graphite–Steam

In this system, catalytic attack by the edge recession mode commenced almost

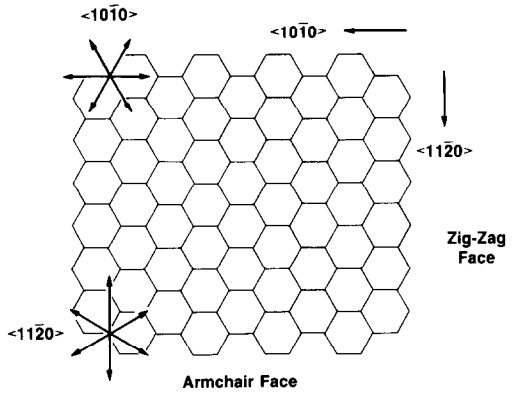

FIG. 1. Miller–Bravais indices of the two principal edges planes of graphite.

immediately following the particle transformation phenomenon described above. This process took place in an ordered fashion, with the edges aligned in directions parallel to the $\langle 11\bar{2}0\rangle$ crystallographic orientations of the graphite. Although edge recession remained the exclusive form of attack over the temperature range studied, a decrease in the rate of edge movement was detected at 920°C and many receding edges came to a complete halt at 1150°C. The spent catalyst could not be reactivated by lowering the temperature; however, if the upper temperature did not exceed 920°C, then the catalyst maintained its activity during a cooling cycle, albeit at a slower rate than that achieved during the initial heating step.

This hysteresis behavior can be seen more clearly from the data presented in Fig. 2. Here the rate of edge recession is plotted against temperature according to the Arrhenius relationship for heating and cooling cycles. From the respective slopes, it is possible to determine that the mean value of the apparent activation energy for the nickel–titanium catalyzed steam gasification of graphite is 33.7 ± 4 kcal/mole^{-1}.

Nickel–Platinum/Graphite–Steam

As with the previous system, edge recession in the presence of nickel–platinum started shortly after the spreading of the particles on the edges of the graphite. It was necessary to raise the temperature to 650°C to obtain measurable rates of reaction. Examination of a number of edges showed that they were either parallel or at 60° to twin bands, i.e., they were oriented in the $\langle 10\bar{1}0\rangle$ crystallographic directions.

The rate of edge recession increased in a systematic fashion as the temperature was progressively increased to 920°C. Provided that this temperature was not exceeded, reproducible edge recession rates were obtained during heating and cooling cycles. A gradual decrease in rate of recession was detected with specimens that were heated to temperatures above 920°C, and this behavior coincided with the appearance of particles at the edge regions. During this phase of the reaction it was not uncommon to find areas of a specimen where both edge recession and channeling were taking place. As the temperature was increased, the incidence of channeling also increased and at 1050°C it became the only form of catalytic attack; and, channeling persisted

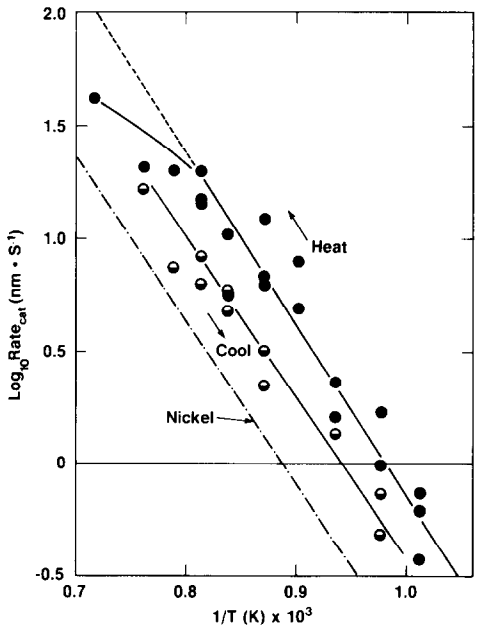

FIG. 2. Arrhenius plots of nickel–titanium-catalyzed graphite–steam reaction during heating and cooling cycles. Also included is the dependence found for nickel (*1*).

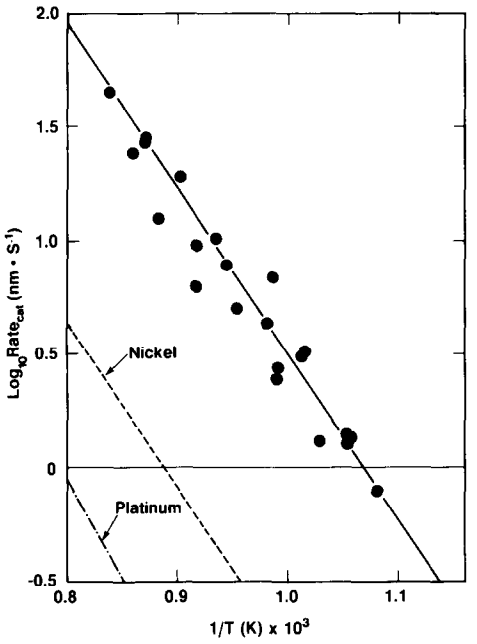

FIG. 3. Arrhenius plot of nickel–platinum-catalyzed graphite–steam reaction. Also included are the dependencies for nickel (*1*) and platinum (*2*).

at temperatures down to 650°C when the specimen was subsequently cooled.

Quantitative kinetic analysis of the edge recession sequences is presented in the form of an Arrehenius plot in Fig. 3, and from the slope of the line an apparent activation energy of 33.2 ± 4 kcal/mole^{-1} can be estimated for the nickel–platinum catalyzed steam gasification of graphite.

Nickel–Ruthenium/Graphite–Steam

The qualitative catalytic influence of nickel–ruthenium on the graphite–steam reaction was identical to that found for nickel–platinum. In the fresh state the bimetallic system operated by the edge recession mode, with the edge movement being parallel to the $\langle 10\bar{1}0 \rangle$ crystallographic orientations, and at high temperatures catalysis occurred by the channeling action. Quantitative kinetic analysis of the edge recession data is presented as an Arrhenius plot in Fig. 4, and from the slope of the line a value of 33.6 ± 4 kcal/mole^{-1} can be estimated for the apparent activation energy of the nickel–ruthenium-catalyzed steam gasification of graphite.

Platinum–Titanium/Graphite–Steam

When this system was heated in 2.0 Torr wet argon, it was necessary to raise the temperature to 515°C to induce particle nucleation. The first sign of catalytic attack of the graphite was seen at 560°C and this took the form of channeling by particles located at edge and step regions. At this stage of the reaction, the width of the channels was 20 to 25 nm, and they tended to follow random pathways.

As the temperature was raised to 625°C, the size of particles which were creating channels increased to 50 nm. It was significant that under these conditions all channels remained parallel-sided throughout their propagation period indicating that there was no tendency for the catalyst material to spread along graphite edges. At 715°C, channels started to become straight

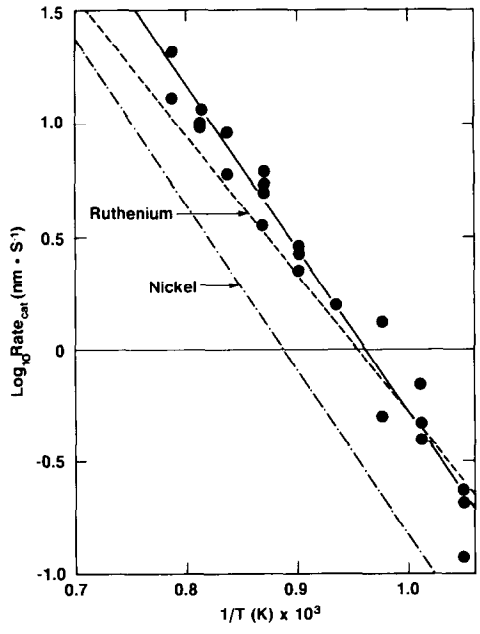

FIG. 4. Arrhenius plot of nickel–ruthenium-catalyzed graphite–steam reaction. Also included are the dependencies for nickel (*1*) and ruthenium (*14*).

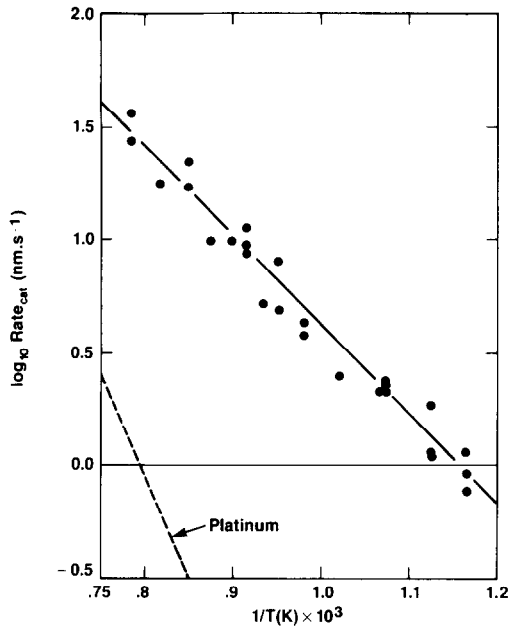

FIG. 5. Arrhenius plot of platinum-titanium-catalyzed graphite–steam reaction. Also included is the dependence found for platinum (*2*).

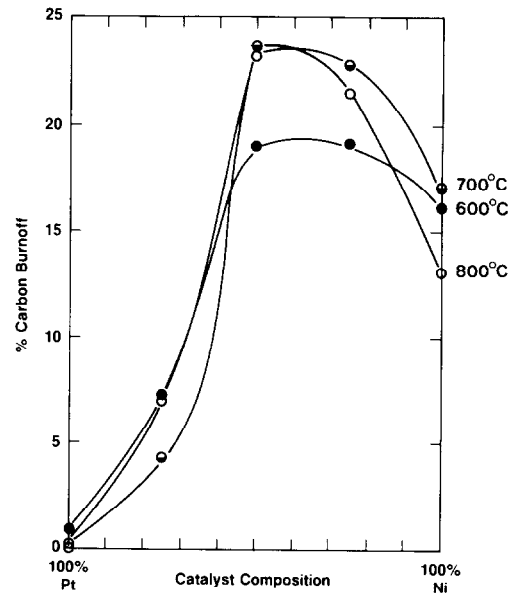

FIG. 6. Percentage carbon burn-off as a function of catalyst composition after 2 h reaction in 0.5% H_2/2.65% H_2O/Ar at 600, 700, and 800°C for the nickel–platinum/graphite system.

and when they changed direction they did so through angles of 60° and 120°. Analysis of many channeling sequences showed that in general their directions were parallel to the $\langle 10\bar{1}0 \rangle$ crystallographic orientations of the graphite. The channels maintained these characteristics up to 1000°C, the highest temperature studied.

An Arrhenius plot of the data obtained from 25-nm-diameter particles cutting channels of similar depth yielded an apparent activation energy of 17.9 ± 2 kcal/mole^{-1} for the platinum–titanium catalyzed steam gasification of graphite, as shown in Fig. 5. Included on this plot for comparison purposes is the dependence found for the influence of similar sized particles of platinum on the same reaction, previously presented in Ref. (*2*).

IV. FLOW REACTOR STUDIES

The data obtained from macroscale experiments with nickel–platinum and nickel–ruthenium on graphite in steam are given in Figs. 6 and 7, respectively. These

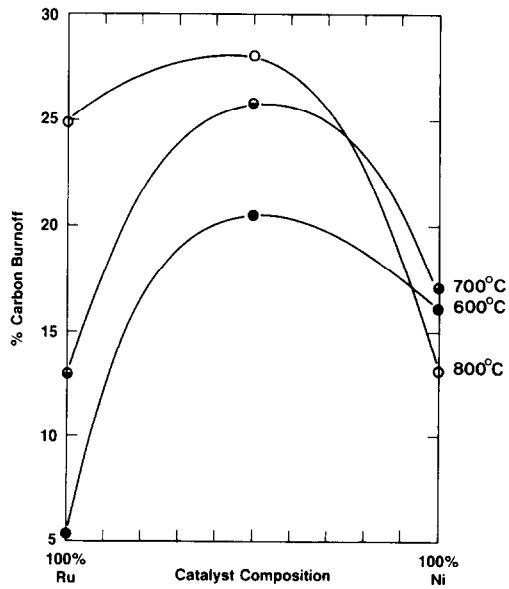

FIG. 7. Percentage carbon burn-off as a function of catalyst composition after 2 h reaction in 0.5% H_2/2.65% H_2O/Ar at 600, 700, and 800°C for the nickel–ruthenium system.

TABLE 1

Comparison of the Rates of Catalytic Attack of Various Bimetallics and Their Pure Components on the Graphite–Steam Reaction at 900°C

	Ni	Pt	Ru	Ti	Cu	Fe
Ni	1.8					
Pt	7.0	0.3*		16.8*		
Ru	6.2		4.3			
Ti	9.5			0.0		
Cu	4.9				0.0	
Fe	16.6*					0.0

Note. The bimetallics are all 50/50 mixtures and the rates (nm · sec^{-1}) are those of edge recession except for Pt, Pt–Ti, and Ni–Fe, which are for channels created by 25-nm-sized particles, and identified by asterisks.

plots show the percentage carbon burn-off of graphite when reacted in a flowing mixture of 0.5% H_2/2.65% H_2O/Ar for 2.0 h, and they clearly demonstrate that addition of a noble metal to nickel can have a profound influence on its catalytic activity for steam gasification of graphite. The activity is higher for catalyst compositions rich in nickel with the optimum being found for catalysts containing equal amounts of nickel and noble metal. Difficulties in preparation of nickel–titanium/graphite and platinum–titanium/graphite specimens on a bulk scale prevented these systems from being studied.

V. DISCUSSION

The idea of enhancing the catalytic activity of a given metal for steam gasification of graphite by the addition of another metal to the catalyst appears to be a viable procedure. Reference to Table 1 shows that the bimetallic systems examined here and in previous CAEM studies all exhibit higher rates of catalytic attack than that of either of their respective pure components. It should be noted that the figures given for nickel–iron and platinum–titanium are for channeling by 25-nm-sized particles, and they are therefore artificially high compared to the edge recession rates of the other bimetallic systems, which has been shown to be a more efficient mode of attack (*5*).

Although it was not possible to determine the surface composition of the catalysts during reaction, using simple thermodynamic considerations in conjunction with solution theory (*6*), it is possible to predict which component in the bimetallic catalyst would be expected to preferentially segregate to the surface in a steam environment. Thermodynamic calculations show that at the steam pressures used in this work, nickel, platinum, and ruthenium will remain in the metallic state, whereas titanium, which has a high affinity for oxygenated species will tend to segregate to the surface of nickel–titanium and platinum–titanium particles. The heat of sublimation of nickel (101.2 kcal/$mole^{-1}$) is much smaller than either platinum (134.8 kcal/$mole^{-1}$) or ruthenium (144.0 kcal/$mole^{-1}$) (*7*), and so in these systems the exposed catalyst surface is expected to be enriched with nickel. A schematic presentation of the postulated behavior of the bimetallic/graphite-steam systems is given in Fig. 8.

To understand the observed changes in the rates of steam gasification of graphite in the presence of bimetallics, one must examine the proposed steps for the metal-catalyzed carbon–steam reaction (*8*).

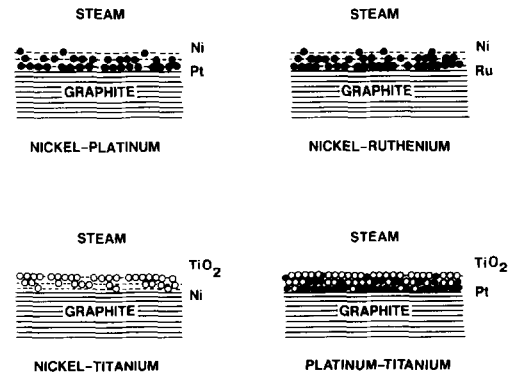

FIG. 8. Schematic representation of the postulated behavior of the various bimetallics on graphite when heated in steam. Ni (---), Pt and Ru (●), and Ti (○).

$$\ldots C{-}C{-}C \ldots + M \rightleftarrows \ldots C{-}C \ldots + M{-}C \quad (I)$$

$$M + H_2O \rightarrow M{-}O + H_2 \quad (II)$$

$$M{-}C + M{-}O \rightarrow 2M + CO \quad (III)$$

The first step in the mechanism is the formation of carbidic carbon on the metal, which depends upon the rupture of a C—C bond in the bulk carbon source, followed by diffusion of carbon species through or over the metal surface. The second step involves the dissociative adsorption of water, and the final step is the formation of CO by reaction of carbidic carbon with adsorbed oxygen species.

The rate-determining step in the nickel-catalyzed steam gasification of graphite is believed to be carbon diffusion through the metal (*9*), (*10*). With platinum, carbon diffusion is rapid (*11*); however, Step II, the dissociation of steam to form Pt—O, does not occur easily (*12*), which explains why this metal is such a poor catalyst for the graphite–steam reaction (*2*). In the nickel–platinum system this constraint is removed due to enrichment of the catalyst surface by nickel. A similar set of arguments can be presented to account for the observed increase in gasification rate of graphite when ruthenium was added to nickel.

Both of these mixed metal systems are excellent examples of bifunctional catalysts where nickel serves as a collector/supplier of oxygen species on the surface and the role of the noble metal is to supply carbon to the catalyst surface. The macroscale experiments clearly show that the maximum gasification activity is achieved with catalyst compositions containing approximately equal amount of the two constituents.

The close agreement in the measured values of the activation energies for the gasification of graphite in the presence of nickel–platinum (33.2 kcal/mole^{-1}), nickel–ruthenium (33.6 kcal/mole^{-1}), and nickel (33.8 kcal/mole^{-1}) point to a common rate-controlling step of carbon diffusion through the nickel component. The presence of Pt and Ru apparently increases the supply of reactive carbon which must subsequently diffuse through Ni and react with surface oxygen.

In the nickel–titanium/graphite–steam reaction the role of nickel is reversed over that when it is mixed with a noble metal. Here the increase in gasification activity of the bimetallic system is probably due to an enhancement in the rate of dissociation of water molecules on the titanium-enriched surface, while nickel increases the supply of reactive carbon. Furthermore, the rate of diffusion of carbon through a nickel–titanium alloy is likely to be faster than through pure nickel; however, some of this influence will be lost at high temperatures due to the formation of a significant fraction of titanium carbide, which will tend to impede the carbon diffusion process. Under the same conditions, carbide formation is not possible with platinum or ruthenium and so deactivation does not occur to the same degree when nickel is mixed with these metals.

With the platinum–titanium/graphite–steam system, the oxidized titanium surface functions as a dissociation center for steam, while the noble metal facilitates the supply of carbon to the reaction site. As a consequence, the mixed catalysts exhibits a much higher activity for the graphite–steam reaction than either of its pure components.

In addition to modifying the catalytic activity of a given metal, introduction of a second element into the system can also produce significant changes in the wetting characteristics of the catalyst on graphite. A striking illustration of this point can be seen from the data presented in Table 2, which is a collection of information from this and previous studies showing the orientation of the catalytic attack as a function of the nature of the catalyst. Of the catalysts listed, platinum, ruthenium, and mixtures containing these metals catalyze gasification in directions parallel to the $\langle 10\bar{1}0 \rangle$ crystallographic orientations or armchair edges,

TABLE 2

Direction and Mode of Attack by Various Catalysts in the Graphite–Steam Reaction

Catalyst	Mode of attack	Orientation of edges developed during catalyzed attack of graphite	Reference
Ca	Edge recession	$\langle 11\bar{2}0\rangle$	*13*
Ba	Edge recession	$\langle 11\bar{2}0\rangle$	*5*
Ni	Edge recession	$\langle 11\bar{2}0\rangle$	*1*
Pt	Channels	$\langle 10\bar{1}0\rangle$	*2*
Ru	Edge recession	$\langle 10\bar{1}0\rangle$	*14*
CaNi	Edge recession	$\langle 11\bar{2}0\rangle$	*13*
CuNi	Edge recession	$\langle 11\bar{2}0\rangle$	*15*
TiNi	Edge recession	$\langle 11\bar{2}0\rangle$	This work
PtNi	Edge recession	$\langle 10\bar{1}0\rangle$	This work
RuNi	Edge recession	$\langle 10\bar{1}0\rangle$	This work
PtBa	Channels	$\langle 10\bar{1}0\rangle$	*2*
PtTi	Channels	$\langle 10\bar{1}0\rangle$	This work

whereas with all the other systems the receding edges are aligned parallel to $\langle 11\bar{2}0\rangle$ orientations or zigzag edges.

In a recent study, Yang and Wong (*16*) used gold decoration to demonstrate that etch pits created by steam in the basal plane of graphite were hexagonal in shape and that the sides of the hexagons were composed of zigzag edges. In contrast, treatment in oxygen or carbon dioxide produced etch pits which were circular. In their initial work on the subject they rationalized these findings according to arguments based on steric factors. They suggested that the linear nature of the oxygen and carbon dioxide molecules precluded the removal of corner carbon atoms in a hexagonal pit causing it to become circular. In contrast, the water molecule being triangular in shape was able to extract the corner carbon atoms and as a result the hexagonal form of the pit was maintained. Further studies have shown that this explanation is incorrect and that dissociative chemisorption of hydrogen, produced during steam decomposition, takes place preferentially at the zigzag edges. This action effectively inhibits reaction of these carbon atoms with steam and, as a consequence, hexagonal pits with zigzag faces are produced (*17*).

Based on these findings it can be assumed that metals which dissociate steam and are left with an oxide or a hydroxide monolayer will preferentially react with the hydroxylated carbon surfaces, i.e., the armchair edges. Of the catalysts listed in Table 2, the alkaline earths and nickel (*18, 19*) fall into this category. In these systems catalytic attack will leave edges orientated parallel to the less reactive $\langle 11\bar{2}0\rangle$ directions, or in a zigzag configuration.

In the case of metals which do not readily dissociate steam, such as the noble metals (*12, 20*), reaction would be expected to occur preferentially with the hydrogenated carbon surfaces, i.e., the zigzag edges. It follows that with the noble metals, and in mixed systems where they tend to segregate at the carbon interface, the residual edges will be aligned along the $\langle 10\bar{1}0\rangle$ directions, or in an armchair configuration.

VI. SUMMARY

In this study we have demonstrated the feasibility of using bifunctional catalysts to enhance the rate of the carbon–steam reac-

tion. In such a mixed catalyst system one component is believed to increase the oxygen reactivity, and the other accelerates the supply of carbon from the source material to the catalyst–gas interface. In addition to modifying the catalytic activity of a given metal, introduction of a second metal into the system can also produce changes in the wetting characteristics of the catalyst on graphite.

REFERENCES

1. Baker, R. T. K., Chludzinski, J. J., Jr., and Sherwood, R. D., *Carbon* **23,** 245 (1985).
2. Lund, C. R. F., Chludzinski, J. J., Jr., and Baker, R. T. K., *Fuel* **64,** 789 (1985).
3. Rao, V. U. S., Szirmae, A., and Fisher, R. M., *J. Catal.* **62,** 44 (1980).
4. Baker, R. T. K., and Harris, P. S., *J. Phys. E* **5,** 793 (1973).
5. Baker, R. T. K., Lund, C. R. F., and Chludzinski, J. J., Jr., *J. Catal.* **87,** 255 (1984).
6. Burton, J. J., Hyman, C., and Fedak, D. G., *J. Catal.* **37,** 106 (1975).
7. Stull, D. R., and Sinke, G. C., "Thermodynamic Properties of the Elements," Advances in Chemistry Series 18. Amer. Chem. Soc., Washington, D.C., 1956.
8. Holstein, W. L., and Boudart, M., *J. Catal.* **75,** 337 (1982).
9. Figueriedo, J. L., and Trimm, D. L., *J. Catal.* **40,** 154 (1975).
10. Baker, R. T. K., and Sherwood, R. D., *J. Catal.* **70,** 198 (1981).
11. Selman, G. L., Ellison, P. J., and Darling, R. S., *Platinum Met. Rev.* **14,** 14 (1970).
12. Fisher, G. B., and Gland, J. L., *Surf. Sci.* **94,** 446 (1980).
13. Baker, R. T. K., and Chludzinski, J. J., Jr., *Carbon* **23,** 635 (1985).
14. Baker, R. T. K., and Chludzinski, J. J., Jr., *J. Phys. Chem.*, in press.
15. Baker, R. T. K., Dudash, N. S., Lund, C. R. F., and Chludzinski, J. J., Jr., *Fuel* **64,** 1151 (1985).
16. Yang, R. T., and Wong, C., *J. Catal.* **82,** 245 (1983).
17. Yang, R. T., and Duan, R. Z., *Carbon* **23,** 325 (1985).
18. Heras, J. M., and Albano, E. V., *Appl. Surf. Sci.* **17,** 207 (1983).
19. Benndorf, C., Nöbl, C., and Madey, T. E., *Surf. Sci.* **138,** 292 (1984).
20. Nieuwenhuys, B. C., *Surf. Sci.* **126,** 307 (1983).